Long-time crossover phenomena in coagulation kinetics

K. Kang* and S. Redner
Center for Polymer Studies and Department of Physics, Boston University, Boston, Massachusetts 02215

P. Meakin
Central Research and Development Department, Experimental Station, E.I. du Pont de Nemours and Company, Wilmington, Delaware 19898

F. Leyvraz
Center for Polymer Studies and Department of Physics, Boston University, Boston, Massachusetts 02215
(Received 18 March 1985)

We employ scaling arguments and numerical simulations to investigate the kinetics of general classes of coagulation processes. Within the rate-equation, or mean-field, approximation, a scaling form for the cluster density is used to predict the asymptotic kinetic behavior for the "product," "sum," and "Brownian" kernels. These predictions are tested by simulations of the particle coalescence model, a model which corresponds exactly to the rate-equation description of coagulation. Our numerical results indicate the presence of an intermediate-time regime of behavior in coagulation kinetics, which is characterized by effective exponents whose values are consistent with scaling. This new and unexpected regime persists for an extraordinarily long time before a crossover to asymptotic behavior sets in. Furthermore, for the sum kernel, our numerical estimates for the exponents which describe the asymptotic kinetic behavior are in disagreement with current theoretical predictions. Finally, new fluctuation-controlled kinetic behavior below an upper critical dimension equal to 2 is also reported.

I. INTRODUCTION

The phenomenon of coagulation, or aggregation, is the basis for a wide variety of kinetic behavior in diverse physical systems, including basic and applied problems such as colloidal and aerosol physics,[1,2] polymer physics,[3,4] studies of antibody-antigen reactions,[5] galactic cluster formation,[6,7] and gelation phenomena.[8–11] Coagulation processes can generally be written in terms of the following reaction scheme:

$$A_i + A_j \xrightarrow{K(i,j)} A_{i+j} .$$

Here A_i denotes a cluster of mass i, and when two clusters of mass i and j meet, they react irreversibly to form a cluster of mass $i+j$ at a rate governed by the rate constant $K(i,j)$. This matrix of rate constants, the reaction matrix, or kernel, embodies the microscopic details of the collision process between two clusters, such as the mass dependence of the collision cross section and the mass dependence of the cluster mobility. In this description of coagulation, the assumption of binary collisions only has been made; this should be a good approximation if the cluster density is small.

The crucial difference between the various physical realizations of aggregation phenomena lies in the functional dependence of the rate constants on the masses of the two incident clusters, i.e., on i and j. This functional dependence of the reaction matrix must usually be derived from a microscopic theory describing the actual system under investigation. Once this functional form is specified, the reaction kinetics can then be treated systematically by studying the Smoluchowski rate equations corresponding to the system. These equations represent an approximation in the spirit of mean-field theory as spatial fluctuations in density are neglected. Therefore, the Smoluchowski equations should provide a valid description of the kinetic behavior, except in low-dimensional systems, where fluctuations effects can be relatively important.

The purpose of this paper is the following. First, in Sec. II, we describe the rate-equation approach to coagulation[8–19] and sketch some basic predictions obtained by assuming a scaling form for the cluster size distribution. Second, we apply the insights gained from this scaling analysis to three important examples of coagulation which are defined by specific forms of the reaction kernel. These examples are the "product" kernel, $K(i,j) \sim (ij)^{\omega}$; the "sum" kernel, $K(i,j) \sim i^{\omega} + j^{\omega}$; and the "Brownian" kernel, $K(i,j) \sim [R(i)+R(j)]^{d-2}[D(i)+D(j)]$, where $R(i)$ is the radius and $D(i)$ is the diffusion constant of a cluster of mass i. The predictions of the scaling theory applied to these kernels will then be tested by numerical simulation approaches in Secs. III and IV.

The bulk of our simulations are based on an idealized model which provides a simple picture for coagulation, the particle coalescence model (PCM).[20] This model has the important feature that an exact correspondence with a specific system of rate equations, defined by the functional form of the reaction kernel, can be made. This equivalence stems from the fact that the rate constants of the PCM can be easily adjusted to take on an arbitrary functional form.

In Sec. III we describe methods by which this PCM may be simulated and also discuss a complementary method, that of numerical integration of the rate equations. Our primary results are then presented in Sec. IV. For the sum and product kernels, our simulations indicate the presence of an unexpected and long-lived intermediate-time regime, in which scaling is apparently satisfied before a crossover to the asymptotic behavior sets in. These interesting crossover effects stem from the very different reaction rates between large clusters with other large clusters, and large clusters with small clusters. However, a full quantitative understanding of the crossover is still lacking. Owing to the surprising results stemming from these simulations, direct numerical integration of the Smoluchowski equations are also performed to serve as a check of the results. Through the use of some computational shortcuts, we are able to integrate the equations to rather long times and thereby support the results from the PCM simulations. For the Brownian kernel, we present results which indicate that the kinetic behavior is quite different than that arising from coagulation with a constant reaction kernel. The kinetic behaviors arising from the two kernels are quite close at short times, but then substantial differences develop at long times.

In Sec. V we perform simulations of the PCM for low-dimensional systems to determine that the upper critical dimension for a wide variety of coagulation phenomena is equal to 2. It should be emphasized that this upper critical dimension refers to the relevance of spatial fluctuations in the cluster densities when the clusters are taken to be pointlike. This critical dimension does not take into account any effects due to the internal geometry of the clusters. Above the upper critical dimension, the rate equations provide an accurate description of coagulation kinetics in the PCM, but in the opposite case, fluctuations in the spatial densities of the reactants give rise to new kinetic behaviors. These new behaviors are readily observable in our simulations, and heuristic arguments are given which yield the observed exponents in the product and sum kernels. Finally, our conclusions are presented in Sec. VI.

II. RATE-EQUATIONS APPROACH

A. The kinetic equation

The mean-field theory of aggregation describes the system in terms of a time-dependent cluster-size distribution, $\{c_k(t)\}_{k=1}^{\infty}$, where $c_k(t)$ is the concentration of clusters of mass k at time t. This description neglects from the outset at least two significant facts: (a) the existence of geometrically different structures for clusters of the same size, and (b) the existence of spatial fluctuations. The former assumption means that a *single* rate constant is used to describe all possible collision processes between i-mers and j-mers. Neglecting the internal cluster geometry can be justified in several ways: If the clusters are fluid droplets, they will always relax after coalescence to a spherical shape. Alternatively, one can arrive at a single rate constant $K(i,j)$ by averaging over all possible geometrical realizations of clusters of mass i and j. While this is hard to justify, it does not seem to be an unreasonable assumption. On the other hand, spatial fluctuations always exist, and with the PCM we can allow for such fluctuations naturally and learn when their influence dominates the long-time kinetics.

Under the two basic assumptions (a) and (b), the rate equations are

$$\dot{c}_k(t)=\tfrac{1}{2}\sum_{j=1}^{k-1} K(j,k-j)c_j(t)c_{k-j}(t) - c_k(t)\sum_{j=1}^{\infty} K(j,k)c_j(t)\ , \tag{1}$$

where the overdot denotes the time derivative. The first term represents the gain of k-clusters owing to the pairwise coalescence of two clusters whose masses add up to k, and the second term represents the loss of k-clusters owing to the coalescence of k-clusters with other clusters.

These equations have been extensively studied, and a relatively large amount of information about the nature of the solutions is known,[8–19] including some exact results for specific forms of the reaction kernel, and more extensive approximate large-time solutions for rather general forms of the reaction kernel. For the purposes of this paper, it will be sufficient to review briefly some of the results from an approximate analysis.

B. Scaling theory and definitions of kinetic exponents

Experiments,[21–23] exact solutions,[8–11] and plausible physical arguments[1,24] all indicate that for large times the solutions to Eq. (1) can be cast into a scaling form,

$$c_k(t)\sim k^{-\theta}\phi(k/s(t))\ , \tag{2}$$

where $s(t)$ is some measure of a characteristic cluster mass. This measure is often taken to be the weight average

$$s(t)=\frac{\sum k^2 c_k(t)}{\sum k c_k(t)}\ . \tag{3}$$

From mass conservation, $\sum_{k=1}^{\infty} k c_k(t)=\text{const}$, one immediately obtains $\theta=2$.

To obtain reasonably complete information about the cluster size distribution, the behavior of $s(t)$ for large times and the behavior of $\phi(x)$ for both small and large values of its argument are required. This last piece of information turns out to be irrelevant, however, since there are virtually no clusters of size $k \gg s(t)$. To describe the behavior of $s(t)$ and of $\phi(x)$ for small x, we define two basic exponents, w and z, as follows:

$$s(t)\sim t^{z}\ \ (t\to\infty)\ ,\qquad \phi(x)\sim x^{w/z}\ \ (x\ll 1)\ . \tag{4}$$

Substituting in Eq. (2) yields

$$c_k(t)\sim k^{-\tau}t^{-w}\ \ [1\ll k\ll s(t),\ t\to\infty]\ , \tag{5}$$

where

$$(2-\tau)z=w\ . \tag{6}$$

Thus w describes the time dependence of the decay of k-mer density, and τ describes the mass dependence of the cluster-mass distribution at fixed time. Finally, a basic exponent α can be defined which describes the time dependence of the total number of clusters,

$$\sum_{k=1}^{\infty} c_k(t)\sim t^{-\alpha}\ . \tag{7}$$

Substituting the scaling form Eq. (5), into Eq. (7), and using the scaling relation (6), we obtain the exponent relations $\alpha=z$ ($\tau\leq 1$) and $\alpha=w$ ($\tau>1$).[24]

To evaluate w and z requires a knowledge of the reaction kernel. For this purpose, we shall consider only kernels which are homogeneous in form; this encompasses essentially all physically relevant situations. Three indices, λ, ν, and μ, may then be introduced to describe the general dependence of the reaction matrix on its two arguments and classify the resulting kinetic behavior.[19] The homogeneity index of the kernel is defined by

$$K(ai,aj)\sim a^{\lambda}K(i,j)\ , \tag{8a}$$

while an index ν may be defined by

$$K(1,j)\sim j^{\nu} \tag{8b}$$

and an index μ may be defined by $\mu=\lambda-\nu$. For $\mu>0$, reactions between the largest clusters predominate over all other types of reactions, while for $\mu<0$, reactions between large-small predominate, and these distinctions give rise to two general classes of behavior.[19] The case $\mu=0$ is marginal, characterized by a balance between the influence of these two types of reactions.

To compute the basic kinetic exponents, we first consider the time dependence of the mass of the typical size cluster. The dominant contribution to this increase arises from aggregates of the typical size reacting with each other. In the spirit of this approximation, the sums appearing in the rate equation for the typical size cluster can be reduced to a single term involving the reaction of two clusters of half the typical size. Taking the second moment of the resulting equation, one immediately finds

$$\frac{ds}{dt}\sim K(s,s)\sim s^{\lambda}\ , \tag{9}$$

leading to the well-known result (see, e.g., Refs. 14 and 17)

$$z=(1-\lambda)^{-1}\ . \tag{10}$$

To evaluate w, we consider the rate equation for $c_1(t)$

$$\begin{aligned}\dot{c}_1(t)&=-c_1(t)\sum_{j=1}^{\infty}K(1,j)c_j(t)\ ,\\ &\sim -c_1(t)\sum_{j=1}^{\infty}j^{\nu}c_j(t)\ ,\\ &\sim -c_1 s^{\nu-1}\int_{s^{-1}}^{\infty}x^{\nu-2}\phi(x)dx\ .\end{aligned} \tag{11}$$

The integral is then either a constant or it is dominated by a divergence at the lower limit. Let us first consider the former case. It then follows that

$$\dot{c}_1(t)\sim -c_1(t)t^{(\nu-1)/(1-\lambda)}\ . \tag{12}$$

Solving for $c_1(t)$ and matching it to the scaling form (2), we deduce that the scaling function must vary as

$$\phi(x)\sim\exp(-x^{\mu})\quad (x\ll 1)\ . \tag{13}$$

That is, the scaling function at small x does not vanish as a power law, as postulated in Eq. (4), but instead vanishes quasiexponentially. This is possible only for $\mu<0$, a condition which is then consistent with the assumed convergence of the integral in Eq. (11). Thus in the case where small-large reactions are most favored, clusters decay according to a quasiexponential law, and w is not defined.

Now consider the opposite case, $\mu>0$, where the integral diverges at the lower limit. Thus in evaluating the discrete sum in Eq. (11), it is sufficient to keep only the first term. That is

$$\sum_{j=1}^{\infty}K(1,j)c_j(t)\simeq c_1(t)\ , \tag{14}$$

and hence, using Eq. (11),

$$c_1(t)\sim 1/t\ , \tag{15}$$

which implies, by Eq. (6),

$$w=1,\quad \tau=1+\lambda\ . \tag{16}$$

An important borderline case arises when $\mu=0$. In this situation, the kinetic behavior appears to depend strongly on the detailed form of the reaction kernel, and relatively little about the general behavior is known.

In the following sections, we shall discuss an example of each of the above three general cases.

(1) $\mu>0$. An important example of this class of reaction kernels is the product kernel, $K(i,j)\sim i^{\omega}j^{\omega}$. This kernel has been used to describe, for example, branched polymerization.[8–11] In such a process, the number of reactive end groups of a branched polymer can increase as a power of the cluster mass. Therefore, the reaction rate between two branched polymers can be modeled by the product kernel. This kernel gives rise to a gelation transition in a finite time for $\omega>\frac{1}{2}$, but we shall focus here on the nongelling case, $0<\omega<\frac{1}{2}$.

(2) $\mu=0$. The example we study here is the sum kernel, $K(i,j)\sim i^{\omega}+j^{\omega}$. This kernel can be used to describe coagulation of Brownian clusters in three dimensions, if the diffusion constants do not depend on the cluster size (see below). No rigorous results are known for the exponents of this model, except for bounds on τ.[25] From the bound $\tau>1$, one has an additional result, $w<z$. Analytical results[14,17] for this kernel are either in disagreement with this rigorous bound or in disagreement with our simulations. This situation points to the subtleties associated with the behavior of a reaction kernel with a characteristic index $\mu=0$.

(3) $\mu<0$. A kernel of this class is the Brownian kernel which is used to describe realistically the detailed collision processes between growing spherical clusters which move by diffusive motion. There exist two competing physical

effects which enter into this reaction kernel. First, more massive clusters will diffuse more slowly, thereby decreasing the rate at which such clusters encounter other clusters. On the other hand, heavier clusters present a larger collision cross section, thereby increasing the reaction rate. These two effects are accounted for by the Brownian kernel,

$$K(i,j)\sim[R(i)+R(j)]^{d-2}[D(i)+D(j)]\ ,$$

where $R(i)$ and $D(i)$ are the radius and diffusion coefficient of a cluster of mass i, respectively. The first factor represents the diffusive flux of a point particle onto a sphere of radius $R(i)+R(j)$. This gives the dependence of the geometrical collision cross section on the cluster radius, under the assumption of spherical clusters. The second factor is the relative diffusivity of two clusters.

For spherical clusters in three dimensions, we have $R(i)\sim i^{1/3}$, while $D(i)$ is proportional to the inverse hydrodynamic radius, a quantity which varies as $i^{-1/3}$. With these identifications, the Brownian kernel can be simplified to

$$K(i,j)\sim(i^{1/3}+j^{1/3})(i^{-1/3}+j^{-1/3})$$
$$=2+(i/j)^{1/3}+(j/i)^{1/3}\ .$$

Thus for this kernel, $\lambda=0$, while $\nu=\frac{1}{3}$, leading to $\mu=-\frac{1}{3}$. Notice also that in a three-dimensional system, if the diffusion constants do not depend on cluster mass, the sum kernel is recovered.

III. NUMERICAL METHODS

A. Particle coalescence model (PCM)

In order to present our numerical results, we first discuss the important new features of our models and simulations that render this investigation practical. First, we employ the recently-introduced particle coalescence model for performing most of our simulations. This simple model describes an idealized coagulation process in which clusters are defined to be *single* lattice sites.[20] When two clusters of mass i and j meet, they coalesce into a heavier single-site cluster of mass $i+j$ at a rate proportional to the reaction kernel, $K(i,j)$. Because there is no cluster geometry, and because we are free to choose the rules for cluster motion, it is possible to specify the reaction matrix in our model *exactly,* and thereby make a precise correspondence with a coagulation process described by a system of rate equations.

The spirit of the PCM model is to describe physical coagulation processes entirely through the functional form of the reaction kernel. Instead of attempting to model faithfully the complicated geometrical effects of aggregating clusters, and then deducing $K(i,j)$, the PCM models $K(i,j)$ directly by algebraic means and neglects the geometry. Thus if a microscopic theory can provide the correct form of $K(i,j)$, then simulations of the PCM model can be used to extract the kinetic behavior. By this approach, we can treat reaction kernels of arbitrary functional form straightforwardly.

This purely kinetic viewpoint of coagulation should be contrasted with the cluster-cluster aggregation model.[24,26–30] Although this model provides a reasonable geometrical representation of real coagulation processes,[26,27] the determination of the reaction kernel for a particular system and the correspondence with the rate-equation approach is a formidable task.[30] In addition, since the geometrical structure of the aggregates is fixed by the imposed model, one does not have the same freedom to choose the reaction kernel as in the PCM. The cluster-cluster aggregation model also assumes that clusters are perfectly rigid and that they do not rotate, assumptions which may not be entirely justified. Attempts to improve on these limitations are quite involved computationally.[31,32] Finally, due to the aforementioned complexities of the cluster-cluster aggregation model, typical simulation results for the kinetics[24,29,30] of this model are several orders of magnitude smaller in scope (both in number of clusters and in number of time steps) than those of the PCM for the same investment of computer time.

B. Simulations of the PCM

We now describe some of the details of the simulation procedure for the PCM. Our primary interest is to develop a method that properly represents the mean-field limit, so that the predictions of the rate equations can be tested numerically. A secondary goal is to simulate coagulation in low-dimensional systems (below the upper critical dimension) in order to investigate the effects of spatial fluctuations.

To simulate the kinetics according to the rate equations, we require that the density of clusters is spatially uniform, and that the relative rate of reaction of an i-mer with a j-mer is strictly proportional to $K(i,j)$. Spatial uniformity is most conveniently achieved by allowing clusters to hop to *any* site of the lattice with the same probability.[33] This equivalent-neighbor hopping rule corresponds to an infinite cluster mobility (on an infinite lattice), and it ensures that mixing effects are as strong as possible, thereby reducing spatial fluctuation effects. An important computational simplification results from equivalent-neighbor hopping because the lattice structure on which the hopping is taking place becomes irrelevant. For simplicity, we have, therefore, performed most of our simulations on a one-dimensional chain.

The effect of the reaction kernel can be most easily accounted for by assigning a sticking probability equal to $CK(i,j)$ when a cluster of mass i meets a cluster of mass j. For kernels with a negative homogeneity index, the constant C may be set equal to unity. However, for positive-homogeneity-index kernels, C must be chosen to be sufficiently small so that the product $CK(i,j)$ remains less than unity during the course of a simulation. The small value of the constant C may be thought of as setting a rather short microscopic time scale.

The primary limiting factor in many of our simulations is the condition that C must be set extremely small in order for the coagulation process to reach large cluster sizes. An alternative approach is to assign a sticking probability $C(t)K(i,j)$, where $C(t)$ is a predetermined monotonically decreasing function of time, chosen so that the sticking

probability remains less than unity throughout the reaction process. This choice for the sticking probability has the advantage of being somewhat more efficient in computer time use, since $C(t)$ can be set fairly close to unity at the initial stages of the reaction. On the other hand, the savings in computer time do not justify the somewhat larger uncertainties that accompany the data obtained in this manner, and we have, therefore, adopted the choice of a sticking probability equal to a small constant amplitude multiplying $K(i,j)$.

With these two rules for cluster mobility and sticking, the detailed simulation procedure is as follows. Initially a given number of monomers are randomly placed on a one-dimensional chain. Then, one by one, a move to an arbitrary lattice site is attempted for each cluster. If this newly chosen site was previously unoccupied, the move is allowed. If the new site was already occupied, a coalescence is defined to occur with probability $CK(i,j)$. If coalescence does not occur, the original cluster is returned to its starting position. This rule is simpler to implement technically than the physically-reasonable alternative of allowing multiple occupancy of sites by unreacted clusters. At large times, or equivalently in the low-density limit, these two alternatives should give the same qualitative results. When all the clusters in the lattice have been moved as just described, the time is increased by one unit, and a new scan through the list of clusters is started.

Superficially, the above method closely resembles the procedure of choosing two clusters at random from a large list of clusters, allowing them to react with probability $CK(i,j)$, and returning the reaction product(s) to the list. Based on this general procedure, a simplified version of cluster-cluster aggregation simulations has been developed.[34] While this method satisfies the basic physical criteria of a mean-field approach, and is also slightly simpler in principle than the PCM, it possesses the drawback that a connection between physical time and the time steps in the simulation cannot be made. Such a connection requires that the cluster density be defined, so that an overall reaction rate can be deduced.

Finally, to investigate the effects of fluctuations in low-dimensional systems, we merely replace the equivalent-neighbor hopping rule with nearest-neighbor hopping. In high dimensions, the kinetic behavior resulting from nearest- and equivalent-neighbor hopping are identical, indicating that fluctuations arising from the diffusive motion of clusters are irrelevant. In lower dimensions, the results from the two hopping rules differ, thereby permitting the investigation of fluctuation-controlled kinetics and the identification of the upper critical dimension.

C. Numerical integration of the rate equations

To help check the validity of simulations of the PCM as a description of the rate equations, we have also performed numerical integrations of the rate equations. Since our primary goal is the extraction of reliable exponent values, and not the accurate evaluation of detailed quantities, we have adapted the standard approach by integrating over very long time intervals for very large systems of equations. By this approach, numerical accuracy has been largely sacrificed, but on the grounds of universality, the exponents characterizing the asymptotic behavior should not be affected in any fundamental way.

To integrate the rate equations, the time is discretized and a cutoff on the number of equations is imposed in order to make the integration numerically tractable. Thus, we replace the rate equations (1) with

$$c_k(t+h)=c_k(t)+h\left[\tfrac{1}{2}\sum_{j=1}^{k-1}K(j,k-j)c_k(t)c_{j-k}(t) - c_k(t)\sum_{j=1}^{N}K(j,k)c_j(t)\right] \qquad (1\le k\le N)\,, \quad (17)$$

where N is the cutoff on the total number of equations to be integrated. As long as the $c_k(t)$ remain positive, these quantities also remain bounded, since it is straightforward to show that

$$\sum_{j=1}^{N} jc_j(t+h) < \sum_{j=1}^{N} jc_j(t)\,. \quad (18)$$

The inequality is due to the production of clusters of masses greater than the cutoff N, which is considered as "loss" of mass in the system. The use of this cutoff, therefore, has the disadvantage of violating mass conservation. This is offset, however, by the fact that no material can accumulate in sizes on the order of N. That is, the cluster-mass distribution behaves smoothly just below the cutoff. On the other hand, if one were to strictly enforce mass conservation by the use of a cutoff in the rate equation of the form

$$\dot{c}_k(t)=\tfrac{1}{2}\sum_{j=1}^{k-1}K(j,k-j)c_j(t)c_{k-j}(t) - c_k(t)\sum_{j=1}^{N-k}K(j,k)c_j(t)\,, \quad (19)$$

then asymptotically the system would reach a final static state in which the remaining clusters of the system would all have masses within the range $N/2$ to N. This finite-size effect makes a mass-conserving cutoff unsuitable for our purposes of studying asymptotic behavior. Thus, we use the cutoff implied in Eq. (17), as this produces a small influence on the kinetics of the concentrations of clusters with masses much less than N.

To reach both very large times and large system sizes, two devices must be used. First it is necessary to use a fast convolution algorithm for the evaluation of the production term. Unfortunately, this leads to the possibility of small negative contributions to some of the cluster concentrations due to round-off errors. This is an early-time effect, however, and it eventually disappears. Second, we adopt the viewpoint that the only really important issue is the stability of the recursion, Eq. (17), where stability means boundedness of the $c_k(t)$'s. We have seen, however, that this is ensured if the $c_k(t)$'s are positive. This latter constraint can be satisfied as long as h is chosen at each time step to be

$$h(t) \lesssim a \left[\max_{1 \le k \le N} \sum_{j=1}^{N} K(j,k) c_j(t) \right]^{-1}, \qquad (20)$$

with $a \lesssim 1$. In practice, we chose a between $\frac{1}{10}$ and $\frac{1}{4}$. With this general procedure, arbitrarily large times can be reached. Due to the cutoff, however, data for times such that the typical cluster size is larger than the cutoff are essentially worthless. To ascertain where this occurs, we monitor the total mass, $\sum_k k c_k(t)$, and discard data when this quantity is less than $\frac{1}{2}$. With these methods, it is not hard to integrate Eqs. (17) with $N=2^{16}$ to $\sim 5\times 10^3$ time units, and beyond, if necessary.

To compare this performance with that of simulations on the PCM, we note that in the PCM, we have typically chosen the initial number of monomers to be of the order of several times 10^5. Thus, in principle, the PCM simulations correspond to integrating this number of equations. In addition, the simulations extend to between 10^5–10^6 time steps. However, this must be rescaled by the constant C in the sticking probability in order to obtain a "physical" time, a quantity which is directly proportional to the time units used in the numerical integration of the rate equations. Since C is generally quite small, the largest time reached in the simulations is of the order of 500 physical time units. The CPU time required for such a simulation is longer than that needed for numerical integration of 2^{16} equations. However, simulations of the PCM manifestly conserve mass and also provide information not available from numerical integration, namely information about large-size clusters.

IV. SIMULATION RESULTS IN THE MEAN-FIELD LIMIT

A. Product kernel ($\mu > 0$)

In order to obtain significant simulation results of equivalent-neighbor hopping in the PCM, it is necessary to choose the constant C in the sticking probability in an optimal way. If C is chosen to be too small, an initial regime of essentially no reaction persists for a relatively long time, and considerable CPU time is wasted. On the other hand, if C is chosen to be larger, then less CPU time is required, but the simulation may have to be terminated before asymptotic behavior sets in because the sticking probability becomes greater than unity. As a typical example, we found that the choice $C=0.0035$ for $\omega=0.25$ was close to optimal for a linear chain of 10^6 sites and an initial monomer density of 0.3.

In Fig. 1(a), we plot the time dependence of the total number of clusters, and of $c_k(t)$ for several values of k. Three general regimes of behavior are observed: First there is the previously mentioned short-time regime where essentially no reaction occurs, due to the extremely small sticking probability of light clusters. Then there follows an intermediate-time regime in which a substantial amount of reaction is occurring. In this regime, which persists for approximately one decade in time, the kinetic exponents α, w, z, and τ can be estimated reasonably well (Table I). Quite strikingly, these estimates disagree with the established asymptotic values of the exponents in Eq.

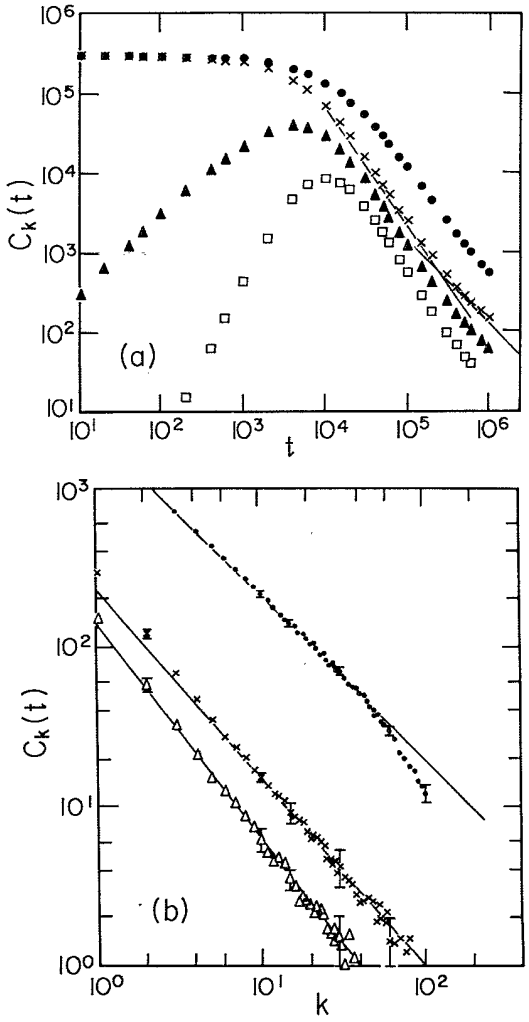

FIG. 1. Typical simulation results for the product kernel, $K(i,j)=Ci^{\omega}j^{\omega}$, simulated by coalescing particles which execute equivalent-neighbor hopping. (a) The dependence of the reaction on the number of time steps in the simulation is illustrated. The number of time steps is related to a physical time by the small multiplicative factor C (see text). Shown are the results from averaging 10 configurations of a linear chain of 10^6 sites with an initial state of 3×10^5 monomers, for $\omega=0.25$ and $C=0.0035$. The symbols refer to the following: ●, the total number of clusters; ×, number of monomers; ▲, number of dimers; □, number of 4-mers. These data are plotted versus the number of time steps on a double logarithmic scale. Notice the crossover from an intermediate-time decay to the asymptotic $1/t$ decay, which is most readily apparent in the behavior of the number of monomers. (b) Dependence of the cluster-mass distribution on mass for fixed times based on averaging over 100 configurations for the same initial conditions as in (a). Plotted is the number of clusters versus mass at 10^4 time steps (●), at 5×10^4 steps (×), and at 10^5 steps (△). The data at 10^4 steps in the mass range 1–30 is linear with a slope of -1.03 as determined by a least-squares fit. Data for larger masses is excluded from the fit, due to the effect of the exponential cutoff. At later times, a similar analysis over the entire range of nonzero data yields a slope approximately equal to -1.23 at 5×10^4 time steps, and a slope of -1.37 at 10^5 time steps. This behavior is indicative of an apparent time dependence in the exponent τ. A number of typical size statistical error bars are shown.

TABLE I. Estimated mean-field values of the kinetic exponents for product-kernel coagulation, $K(i,j)\sim i^{\omega}j^{\omega}$, with $\omega=0.25$ and 0.40, obtained from simulations of the particle coalescence model. Estimates have been given for both the transient intermediate-time regime and the asymptotic regime, as discussed in the text. For the purposes of comparison, the accepted analytical expressions for the kinetic exponents are given as well.

		This work			
		$\omega=0.25$		$\omega=0.40$	
	Theory[a]	($t\lesssim 10^4$) intermediate	($t\gtrsim 10^4$) asymptotic	($t\lesssim 10^4$) intermediate	($t\gtrsim 10^4$) asymptotic
α	1	1.4	1.1	1.5	1.2
w	1	1.5	1.0	1.6	1.1
τ	$1+2\omega$	0.95	1.4	1.3	1.7
z	$1/(1-2\omega)$	1.4	1.9	2.4	4.0

[a]See, e.g., Refs. 14 and 25.

(16), but they are internally consistent with the scaling relation Eq. (6). This peculiar result may be of considerable experimental relevance, as scaling is apparently satisfied over a reasonable temporal range, but with the "wrong" exponents.

Finally, after a rather long time, a crossover to a different kinetic behavior occurs. As shown in Fig. 1(a), this crossover is most readily apparent in the density of the smallest clusters, as the asymptotic regime for this size range sets in the soonest. In the asymptotic regime, the exponents are consistent with scaling, and also in agreement with the asymptotic predictions of Leyvraz.[14]

Some insights into the origin of the intermediate-time regime can be gained by pursuing the most simple-minded consequences of a scaling form for the cluster density. Thus we substitute the scaling form, Eq. (2), into the rate equations, and then investigate the possible kinetic behaviors by imposing a number of drastic but highly simplifying assumptions. Since we are interested primarily in the long-time, small-mass limit, the effects of the finite number of production terms (first factor) in the rate equation are neglected. This is justified since these terms make only a negligible contribution at long times compared to the infinite number of loss terms in the rate equations. In addition, the sums in the rate equations are replaced by integrals. With these steps, it is relatively straightforward to verify that three possible generic classes of behavior are possible which are delineated by different ranges of values for τ. The origin of these three classes depends crucially on the value of τ, as this exponent governs whether various moments of the cluster size distribution, which eventually enter in the procedure of substituting the scaling form (2) into (1), converge or diverge. The three classes of behavior are characterized by the following sets of kinetic exponents.

$$\alpha=z=1/(1-\omega),\quad 0<\tau\leq 1 \tag{21a}$$

$$\alpha=w,\quad z=1/(1-\omega),\quad 1<\tau<1+\omega \tag{21b}$$

$$\alpha=w=1,\quad 1+\omega\leq\tau\,. \tag{21c}$$

To compare these predictions with the simulation results, note that the intermediate-time estimate of τ for $\omega=0.25$ is less than unity, corresponding to behavior of (21a). Our simulation results for $\omega=0.25$ are in reasonable agreement with (21a), and furthermore, the observed exponents are internally consistent with scaling (Table I). Similarly, for $\omega=0.40$, the simulation results appear to fall into the general class of behavior given in (21b). Once again the data are in reasonable agreement with (21b), and they are also internally consistent with scaling. However, the exponents in (21a) and (21b) are incorrect asymptotically, as more detailed analyses of the rate equations have demonstrated.[14,19] Only in the case where $\tau\geq 1+\omega$, does the simple-minded substitution of the scaling form in the rate equations give the correct asymptotic results.

Thus the gradual crossover appears to originate mathematically from the fact that the cluster-size exponent τ is time dependent. Evidence for this striking phenomenon can be seen in Fig. 1(b), where we plot $c_k(t)$ versus k at various times. For relatively short times (number of steps $\lesssim 10^4$), one clearly observes a power-law decay for small k, with an effective exponent τ approximately equal to 1. For values of k larger than the typical cluster size, this power-law decay is then sharply cut off as embodied by the scaling form (2). At larger values of the time, the power-law regime for $c_k(t)$ persists to larger masses, as expected by scaling. However, quite surprisingly, the slope of the power-law regime is getting gradually steeper as well.

The physical origin for this crossover seems to stem from the much larger reaction rate for massive clusters than for light clusters. In the intermediate-time regime, enough reaction is occurring so that the cluster-size distribution establishes an apparent power-law decay, but very large clusters have not yet had time to form. However, once sufficiently large clusters do form, they will react at a very high rate. Thus the large-mass portion of the cluster-size distribution will be quickly depleted, while the small-mass tail will tend to persist. Evidently, the combined effect of these two features is to steepen the cluster-size distribution, thereby giving rise to the ostensible time dependent of τ [Fig. 1(b)].

B. Sum kernel ($\mu=0$)

To simulate the sum kernel, $K(i,j)\sim i^{\omega}+j^{\omega}$, we proceed as in the case of the product kernel and assign a

sticking probability equal to $C(i^\omega+j^\omega)$ when two clusters of mass i and j meet. Upon performing fairly large-scale simulations based on this approach, a rather disturbing result is found. For both $\omega=0.25$ and $\omega=0.40$, the cluster-size exponent τ is apparently less than unity (Table II). However, rigorous bounds[25] have recently been derived which state that τ must be greater than unity for any positive value of ω. Our conclusion, then, is that the observed behavior is not the asymptotic one, as in the product kernel, but that the crossover time for the asymptotic behavior is beyond the range of the simulation.

To understand these disturbing results, we performed

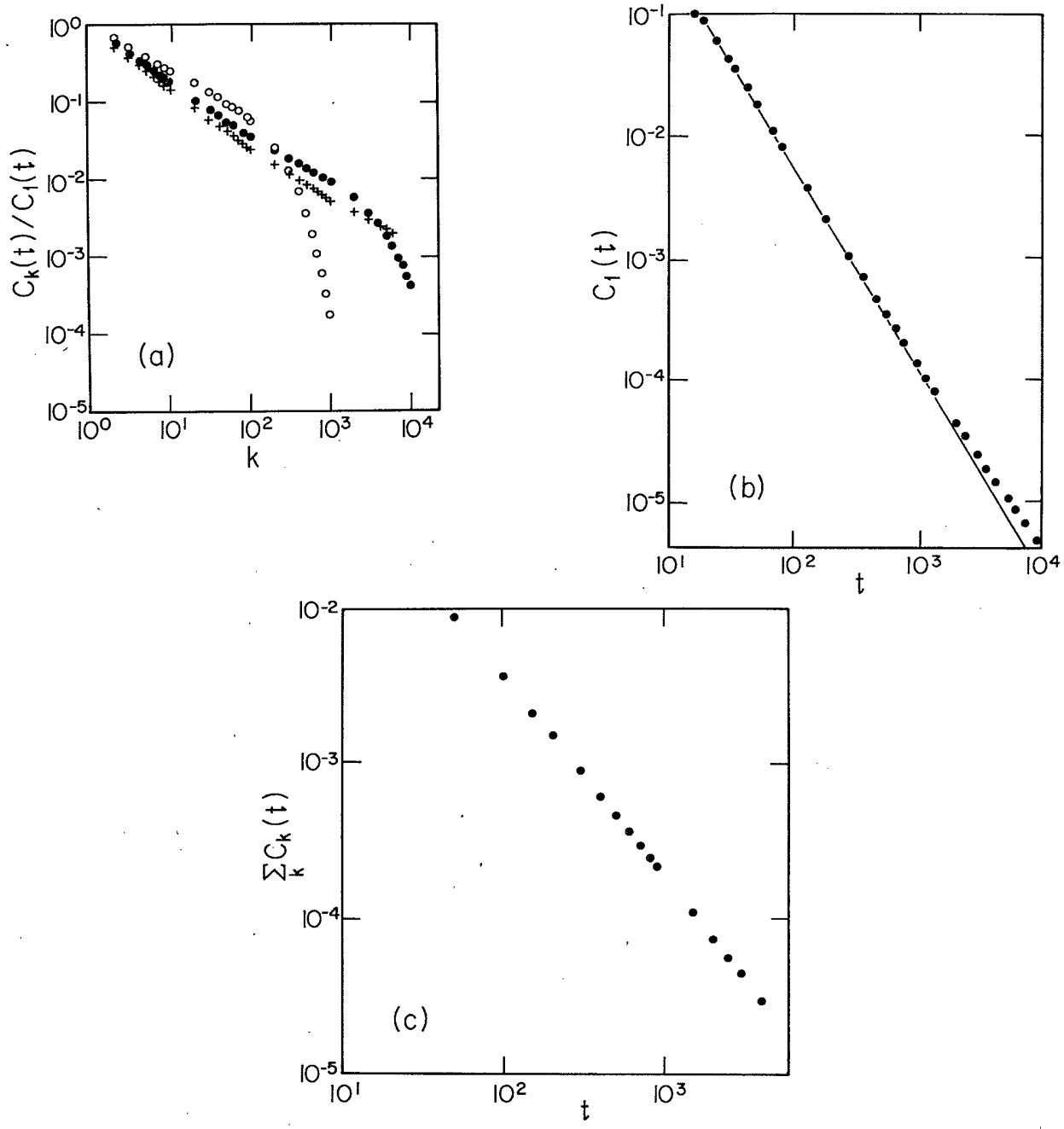

FIG. 2. Typical results from the sum kernel, $K(i,j)\sim i^\omega+j^\omega$, from a numerical integration of the rate equations. Shown are the results from integrating 65 536 equations for up to 5×10^3 time units. These units correspond directly to a physical time. In (a) we plot the quotients $c_k(t)/c_1(t)$ versus k at 50 time units (○), at 500 time units (●), and at 2000 time units (+) in order to show the slow approach to an "equilibrium" state where the quotients are time independent. The initial slope of the data is approximately -0.62 at 50 time units, increasing gradually to -0.83 at 2000 time units. Notice also the presence of a slight curvature in the data for masses less than the cutoff. In (b) we plot $c_1(t)$ versus the number of time units to show the evidence for the beginnings of a crossover only after $\gtrsim10^3$ time units have elapsed. (c) Finally we plot $\sum_k c_k(t)$ versus the number of time units. These data suggest that $\alpha\cong z=1.33$, consistent with both $\tau<1$ and with scaling, but these exponents are known to be incorrect asymptotically.

TABLE II. Estimated mean-field values of the kinetic exponents for the sum kernel, $K(i,j)\sim i^{\omega}+j^{\omega}$, for $\omega=0.25$, 0.40, and 0.75 from simulations of the particle-coalescence model, and comparison with the theoretical predictions. For $\omega=0.25$ and 0.40, the rigorous bound $\tau>1$ (Ref. 25) is not satisfied and the quoted exponents are, therefore, not characteristic of asymptotic behavior.

		This work		
	Theory[a]	$w=0.25$	$w=0.40$	$w=0.75$
α	$=w$	1.29	1.53	2.5
w	$<z$	1.76	1.75	2.5
τ	>1	0.63	0.84	1.3
z	$1/(1-\omega)$	1.32	1.56	3.3

[a]See, e.g., Ref. 25.

numerical integration of the rate equations for $\omega=0.25$, for $N=65\,535$ equations, going up to $t\simeq 5\times 10^3$ time steps. To present our results, we note that if the asymptotic form

$$c_k(t)\sim k^{-\tau}t^{-w}\,, \tag{22}$$

valid for $t\to\infty$ and $1\ll k\ll s(t)$, is reached, then the quotients $c_j(t)/c_1(t)$ are time independent, at least for sizes $k\ll s(t)\sim t^z$. These quotients are plotted in Fig. 2(a) for a number of different values of k between 1 and 100, and it is readily seen that they settle to an equilibrium value only extremely slowly. Furthermore, the value of τ characterizing the cluster-mass distribution apparently varies smoothly from approximately 0.60 to 0.8 as shown in the figure. The smaller values of τ found from the numerical integration also agree with the values obtained in simulations of the PCM in the time range where the two simulations could be directly compared.

A plot of $c_1(t)$ versus time is shown in Fig. 2(b). A power-law decay of $c_1(t)$ apparently holds over a substantial temporal range, but the decay slows down at longer times. This slowing down cannot be taken as conclusive evidence of a crossover, however, since at the time where the slower decay sets in, finite size effects are quite noticeable. In particular, for $t>1200$ time units, the second moment decreases with time.

The value of w which can be extracted from this data (both at intermediate and at long times) are in disagreement with the theoretical predictions of Leyvraz[14] and Botet-Jullien.[17] More problematic is that through the whole range of times investigated, the rigorous relations $\tau>1$, and hence $w<z$ as well as $\alpha=w$, are all violated. We do not know of a satisfactory explanation for these facts.

C. Brownian kernel ($\mu<0$)

In the classical treatments of Brownian coagulation, the mass-dependent terms were neglected,[12,13] so that the kinetics is reduced to that of constant-kernel coagulation. This is a reasonable approximation at the early stages of the reaction, where large clusters have not yet had time to form. However, as discussed in Sec. II, the Brownian kernel is dominated by large-small reactions, and these become rather important at the later stages of the coagulation process.

To illustrate this crossover, we have simulated Brownian kernel coagulation on a one-dimensional chain of 5×10^5 sites (Fig. 3). In close analogy with the simulations of the product and sum kernels, we must also model the reaction kernel in terms of a mass-dependent sticking probability, and use the infinite-mobility hopping rule. For this purpose, we again multiply the reaction kernel by a small constant to ensure that the product,

$$C\,K(i,j)=C[2+(i/j)^{1/3}+(j/i)^{1/3}]\,,$$

which is the sticking probability in our simulation method, will always be less than unity. For the simulation results shown, we found that the choice $C=0.08$ was close to optimal. We observe that the total number of clusters decays as $1/t$ over a very large range in time, a behavior identical to that of constant-kernel coagulation. During the initial stages of decay, the individual cluster populations decrease as $1/t^2$, as in constant kernel coagulation. However, there is a crossover to a much steeper decay which appears to be quasiexponential at longer times. It does not seem possible to compare the data quantitatively with Eq. (13) unless a considerably larger system could be simulated so that data could be taken

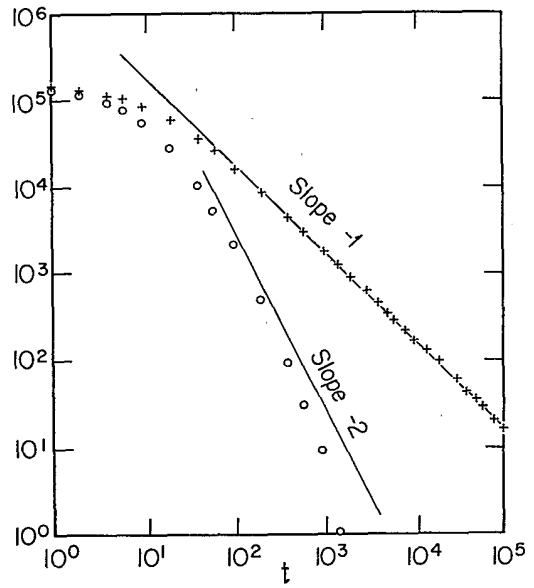

FIG. 3. Typical results for the Brownian kernel, $K(i,j)=C[2+(i/j)^{1/3}+(j/i)^{1/3}]$, from simulations of the particle coalescence model with equivalent-neighbor hopping. Shown are the results from a linear chain of 5×10^5 sites with an initial state of 1.5×10^5 monomers, and with $C=0.08$. The data for the total number of clusters (+), plotted versus the number of time steps on a double logarithmic scale, lie approximately on a straight line of slope -1, indicating that the exponent $\alpha=1$. The data for the monomer number (○) initially appear to be decaying as $1/t^2$, but asymptotically the decay is faster than a power law.

over a more extensive range in time. Nevertheless, the available evidence indicates the existence of the expected crossover.

V. SIMULATION RESULTS BELOW THE UPPER CRITICAL DIMENSION

The results of the previous section have been obtained on the basis of simulations of models in which density fluctuations are negligible. However, for low-dimensional systems, where diffusive transport can be described in terms of nearest-neighbor or short-distance hopping, spatial fluctuations can occur and dramatically influence the kinetic behavior. In particular, it has been determined previously that for constant-kernel coagulation, the upper critical dimension d_c equals two,[20] and that logarithmic corrections to the mean-field behavior can be observed in two dimensions.

In this section, we study the product and sum kernels in low dimensions in order to ascertain the upper critical dimension for these systems, and to study the kinetics below this upper critical dimension. To this end, we compare the dimension-independent (mean-field) simulation results based on the equivalent-neighbor hopping rule, with the results based on local hopping rules, for the same reaction kernel. In three dimensions, we find, for the sum and product kernels, that the results from the local hopping rules are essentially identical to those obtained from equivalent-neighbor hopping. In two dimensions, the results of the two hopping rules no longer coincide exactly, but are quite close. This seems to be indicative of a relatively small (possibly logarithmic) difference between the two sets of results, in analogy with the results from constant-kernel coagulation.[20] Finally, in one dimension, the results of the two hopping rules are completely different. From this general picture, we identify two as the upper critical dimension for coagulation kinetics when clusters move by Brownian motion. A more thorough verification of this assertion could be obtained by performing simulations of coagulation on fractal lattices in which the fracton dimension is between one and two.

It appears that the underlying physical mechanism for the upper critical dimension is the transition from recurrence to transience for random walks, a transition which occurs in two dimensions. Below two dimensions, the recurrence of random walks guarantees that clusters are more likely to collide with near neighbors, rather than with distant neighbors, and fluctuation effects can become important. In the opposite case, the transience of the random-walk motion ensures that a particular cluster has essentially the same probability of reacting with any other cluster in the system, i.e., the mean-field limit.

In simulations of the product kernel by the PCM, we continue to use a mass-dependent sticking probability, but with nearest-neighbor cluster hopping. In one dimension, the results suggest that the asymptotic kinetics is independent of the value of ω, and we estimate $\alpha=z=\frac{1}{2}$ [Fig. 4(a)]. This behavior is reminiscent of the situation encountered in bimolecular decay when recombination occurs with a very small (constant) reaction probability.[33] It was found that the asymptotic kinetics is independent of the sticking probability when the system is below the upper critical dimension. Apparently, a similar phenomenon appears to be occurring in product kernel coagulation.

To model the sum kernel, we note that it is of the form $[D(i)+D(j)]$, where $D(i)\sim i^{\omega}$ can be thought of representing a mass-dependent diffusion constant of a cluster of mass i. There are several ways that such a mass-dependent diffusion coefficient can be simulated nu-

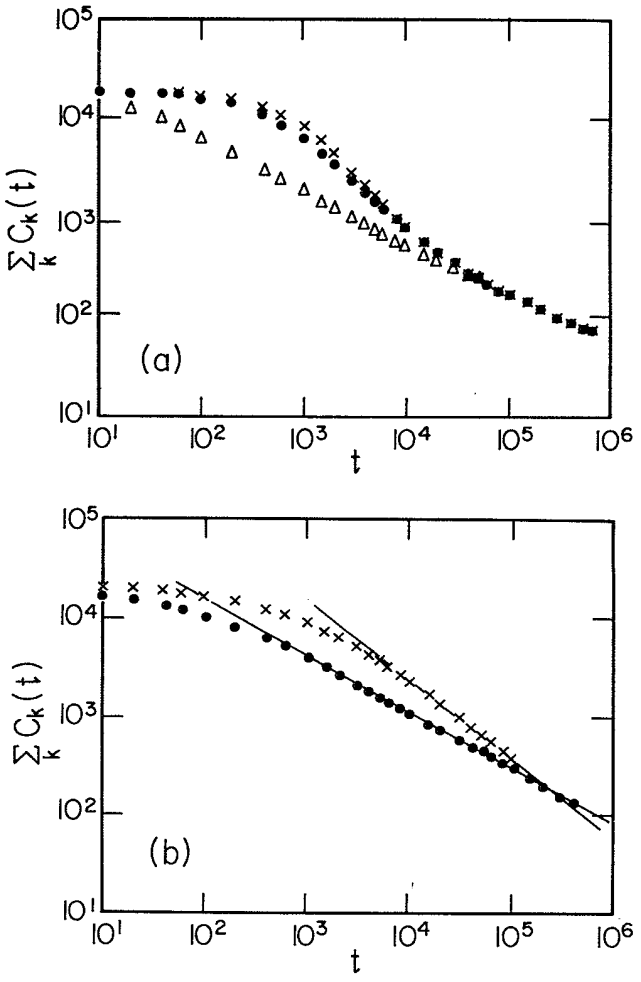

FIG. 4. Simulation results below the upper critical dimension for (a) the product and (b) the sum kernels. Plotted are the total number of clusters as a function of the number of time steps based on simulations of particle coalescence on a chain of 10^5 sites, in which clusters move by nearest-neighbor hopping. For the product kernel, the cases $\omega=0.10$ (△), 0.25 (●), and 0.50 (×) are shown, in which the multiplicative constant $C=0.2$, 0.01, and 0.005, respectively. Asymptotically, all the data lie on a common straight line of slope $-\frac{1}{2}$. For the sum kernel, the cases $\omega=0.25$ (●) and 0.75 (×) are shown, with $C=0.15$ and 0.02, respectively. The slopes of the straight lines which pass through the data points at large times are 0.56 and 0.77, respectively. These numbers compare well with our theoretical predictions of 0.571... and 0.80, respectively, for these two cases.

merically. One possibility is to move each cluster i^ω steps in a random walk, while a second alternative is to allow a cluster to take a single random step with a probability proportional to i^ω. Both approaches give essentially identical results, thereby providing a useful check of the methods. Applying these two methods in one dimension, we find that τ is negative, leading to a population inversion in the cluster-size distribution as a function of mass.[29] These results are also quite similar to those found in constant-kernel coagulation in one dimension.[20] The value of τ is found to increase as ω increases, reaching the value $\tau=0$ when $\omega=1$. This special case, $\omega=1$, appears to display the same behavior as constant-kernel coagulation in the mean-field limit.

A simple, but very heuristic argument can be given to predict some of the kinetic exponents of sum-kernel coagulation below the upper critical dimension. It is known that for constant-kernel coagulation, $\sum_k c_k(t)$ is proportional to $(Dt)^{-d/2}$ for spatial dimension $d<d_c=2$, where D is the diffusion coefficient. For the sum kernel, D is now mass dependent, varying as i^ω for a cluster of mass i. When a distribution of cluster sizes is present, we, therefore, write

$$\sum_k c_k(t) \sim (\langle D \rangle t)^{-d/2} \sim (\langle k^\omega \rangle t)^{-d/2} \sim (t^{\omega z+1})^{-d/2} .$$

From the definition of α, and the scaling relation $\alpha=z$ for $\tau<1$ (as observed in our simulations), we have $z=(\omega z+1)d/2$. This leads ultimately to $\alpha=z=d/(2-\omega d)$, in excellent agreement with our numerical data [Fig. 4(b)].

VI. CONCLUSIONS

In summary, we have found that the kinetic behavior of a variety of aggregation phenomena are not simply described by the asymptotic solutions of the Smoluchowski rate equations. These findings are primarily based on numerical simulations of the particle coalescence model, an idealized model which, above an upper critical dimension equal to 2, corresponds exactly to the Smoluchowski rate equations. This upper critical dimension signals the regime where fluctuations in the spatial density of the clusters may be neglected.

In the particle coalescence model, the essential kinetic aspects of coagulation are described in terms of the density of pointlike clusters, while complicated geometrical effects, such as the influence of cluster structure on the reaction rate, are simply absorbed into the functional form of the reaction kernel. Since the rate constants can be chosen to have an arbitrary functional form, and through the equivalence between the model and the rate equations, we are in a position to study a wide variety of coagulation phenomena over the entire temporal range.

For both the product and sum kernels, a new intermediate-time regime, with effective exponents consistent with scaling, is observed. For the product kernel, there is an eventual crossover at long times to a distinct asymptotic behavior, which is in agreement with theoretical predictions based on solutions to the Smoluchowski equations. In the case of the sum kernel, the predicted crossover to asymptotic behavior occurs beyond the range accessible by simulations of the particle coalescence model, and also by numerical integration of the rate equations. With the latter method, we do find that the scaling form for the cluster-size distribution sets in only extremely slowly. This points to the fact that the kinetics of sum-kernel coagulation is quite subtle. For the Brownian kernel, we have seen that the kinetic behavior is very close to that of constant-kernel coagulation at short times. However, at larger times, reactions of small clusters with large clusters predominate, and $c_k(t)$ decays at a more rapid quasiexponential rate, rather than as $1/t^2$ as in the constant-kernel case.

Our simulation results may be of experimental relevance,[21–23] as it appears that the true asymptotic behavior to the Smoluchowski equations may not be observed until very long times have elapsed, a time regime which may be beyond the range of typical experimental probes. The detailed understanding of this long-time crossover effect remains an interesting open question.

ACKNOWLEDGMENT

The Center for Polymer Studies is supported in part by grants from the U.S. Army Research Office, NSF, and U.S. Office of Naval Research.

*Deceased.

[1]S. K. Friedlander, *Smoke, Dust and Haze: Fundamentals of Aerosol Behavior* (Wiley, New York, 1977); S. K. Friedlander and C. S. Wang, J. Colloid Interface Sci. **22**, 126 (1966).

[2]R. L. Drake, in *Topics in Current Aerosol Research,* edited by G. M. Hidy and J. R. Brock (Pergamon, New York, 1972), Vol. 3, Part 2.

[3]P. J. Flory, *Principles of Polymer Chemistry* (Cornell University Press, Ithaca, New York, 1977), pp. 317–398.

[4]W. H. Stockmayer, J. Chem. Phys. **11**, 45 (1943).

[5]F. W. Wiegel and A. S. Perelson, J. Stat. Phys. **29**, 813 (1982); A. S. Perelson and R. W. Samsel, in *Kinetics of Aggregation and Gelation,* edited by F. Family and D. P. Landau (North-Holland, Amsterdam, 1984).

[6]G. B. Field and W. C. Saslaw, Astrophys. J. **142**, 568 (1965).

[7]J. Silk and S. D. White, Astrophys. J. **223**, L59 (1978).

[8]F. Leyvraz and H. R. Tschudi, J. Phys. A **14**, 3389 (1981).

[9]F. Leyvraz and H. R. Tschudi, J. Phys. A **15**, 1951 (1982).

[10]E. M. Hendriks, M. H. Ernst, and R. M. Ziff, J. Stat. Phys. **31**, 519 (1983).

[11]M. H. Ernst, R. M. Ziff, and E. M. Hendriks, J. Colloid Interface Sci. **97**, 266 (1984).

[12]M. V. von Smoluchowski, Phys. Z. **17**, 557 (1916).

[13]S. Chandrasekhar, Rev. Mod. Phys. **15**, 1 (1943).

[14]F. Leyvraz, Phys. Rev. A **29**, 854 (1984).

[15]R. M. Ziff, in *Kinetics of Aggregation and Gelation,* edited by F. Family and D. P. Landau (North-Holland, Amsterdam, 1984).

[16]A. A. Lushnikov, J. Colloid Interface Sci. **46**, 549 (1973); **48**, 400 (1974); **54**, 94 (1975).

[17]R. Botet and R. Jullien, J. Phys. A **17**, 2517 (1984).
[18]M. H. Ernst, E. M. Hendriks, and F. Leyvraz, J. Phys. A **17**, 2137 (1984).
[19]P. G. J. van Dongen and M. H. Ernst, Phys. Rev. Lett. **54**, 1396 (1985).
[20]K. Kang and S. Redner, Phys. Rev. A **30**, 2833 (1984).
[21]Z. Djordjevic, Ph.D. thesis, Massachusetts Institute of Technology, 1984.
[22]J. Feder, T. Jossang, and E. Rosenquist, Phys. Rev. Lett. **53**, 1403 (1984).
[23]D. A. Weitz, J. S. Huang, M. Y. Lin, and J. Sung, Phys. Rev. Lett. **53**, 1657 (1984).
[24]S. K. Friedlander and C. S. Wang, J. Colloid Interface Sci. **22**, 126 (1966); T. Vicsek and F. Family, Phys. Rev. Lett. **52**, 1661 (1984); in *Kinetics of Aggregation and Gelation,* edited by F. Family and D. P. Landau (North-Holland, Amsterdam, 1984).
[25]P. G. J. van Dongen and M. H. Ernst, Phys. Rev. A **32**, 670 (1985).
[26]P. Meakin, Phys. Rev. Lett. **51**, 1119 (1983).
[27]M. Kolb, R. Botet, and R. Jullien, Phys. Rev. Lett. **51**, 1123 (1983).
[28]M. Kolb, Phys. Rev. Lett. **53**, 1653 (1984).
[29]P. Meakin, T. Vicsek, and F. Family, Phys. Rev. B **31**, 564 (1985).
[30]R. M. Ziff, E. D. McGrady, and P. Meakin, J. Chem. Phys. **82**, 5269 (1985).
[31]P. Meakin, J. Chem. Phys. **81**, 4637 (1984).
[32]P. Meakin and R. Jullien, J. Phys. (Paris) **46**, 1543 (1985).
[33]K. Kang and S. Redner, Phys. Rev. A **32**, 435 (1985).
[34]R. Botet, R. Jullien, and M. Kolb, J. Phys. A **17**, L75 (1984); Phys. Rev. A **30**, 2150 (1984).